Beamforming Design for Secure SWIPT Systems Under a Non-linear Energy Harvesting Model

Elena Boshkovska[1], Nikola Zlatanov[2], Xiaoming Chen[3], Derrick Wing Kwan Ng[4] and Robert Schober[5]

[1,5]*Friedrich-Alexander-University Erlangen-Nuremberg (FAU), Germany*

[2]*Monash University, Australia*

[3]*Zhejiang University, P.R. China*

[4]*The University of New South Wales, Australia*

Abstract: Simultaneous wireless information and power transfer (SWIPT) is an appealing solution to extend the lifetime of wireless nodes and hence alleviate the energy bottleneck of energy-constrained wireless communication networks. SWIPT advocates the dual use of radio frequency signals for conveying information and energy concurrently which introduces a paradigm shift in system design. This chapter focuses on the use of multiple antennas to improve the efficiency of wireless power transfer (WPT) and secure information transmission. In particular, our objective is to maximize the secrecy rate of a SWIPT system via beamforming. To this end, we formulate a non-convex optimization problem based on a practical non-linear energy harvesting model. The problem formulation allows for the use of an energy signal to improve WPT efficiency and to provide communication security. The globally optimal solution of the design problem is obtained via a one-dimensional search and semidefinite programming (SDP) relaxation. Numerical results demonstrate that the proposed design can achieve a significant gain in secrecy rate compared to two baseline schemes.

Keywords: Beamforming, non-linear energy harvesting, wireless information and power transfer, secure communication.

1. Introduction

Wireless sensor networks serve as a key enabler of the Internet-of-Things (IoT) [1], which connects a tremendous number of sensors to computing systems to provide intelligent daily life services such as e-health, automated control, energy management (Smart City and Smart Grid), logistics, security control, and safety management, etc. The European Commission has predicted that by 2020, there will be 50 to 100 billion devices connected to the Internet. In general, wireless sensors are small devices powered by batteries with limited energy storage capacity. Hence, the re-

sulting limited lifetime of wireless sensor networks is foreseen to be a fundamental system performance bottleneck for the deployment of IoT. Conventionally, battery replacement provides an intermediate solution to energy depletion which is suitable for networks with small numbers of devices. However, frequent replacement of batteries in IoT networks with massive numbers of sensors is costly and cumbersome. Besides, in some application such as biomedical implant senors, it is almost impossible to replace sensor batteries once they are deployed. More importantly, battery replacement may create temporary service suspension which is not possible in systems requiring stable communication services. Therefore, different promising approaches/technologies, such as energy efficiency optimization [2, 3], energy harvesting technology [4]–[7], and cooperative communications [8, 9], have been proposed to extend the lifetime of wireless communication networks. Energy harvesting is particularly appealing as it provides self-sustainability to wireless communication networks. Thereby, wireless communication devices are equipped with energy harvesting technology to collect energy from the environment. Solar, wind, tidal, biomass, and geothermal are the major candidate renewable energy sources for generating electricity [4, 5]. Yet, these conventional natural energy sources are usually only available at specific locations which limits the mobility of the devices. Besides, theses sources are also climate dependent. Hence, the intermittent and uncontrollable nature of these natural energy sources makes it difficult to integrate conventional energy harvesting technology into wireless communication devices.

Wireless power transfer (WPT) has attracted much attention from both academia and industry [10]–[26], recently, as a building block for the IoT. The existing WPT technologies can be categorized into three classes: inductive coupling, magnetic resonant coupling, and radio frequency (RF)-based WPT. In general, compared to the aforementioned conventional energy sources, WPT can provide regular and controllable energy supply. Also, if the locations of the energy harvesting nodes are fixed, the amounts of average harvested wireless power at the receivers are predictable since the WPT efficiency depends mainly on distance. Inductive coupling and magnetic resonant coupling technologies rely on near-field electromagnetic (EM) waves. Hence, they cannot support the mobility of energy harvesting devices, due to the limited wireless charging distances and the required alignment of the EM-field with energy harvesting circuits. In contrast, RF-based WPT [10]–[26] exploits the far-field properties of EM waves to convey wireless energy. The use of RF for WPT in communication systems enables the possibility of simultaneous wireless information and power transfer (SWIPT) leading to a paradigm shift in system architectures and designs. In particular, SWIPT systems can exploit the broadcast nature of the wireless medium to facilitate one-to-many wireless charging and wireless communication which may not be possible when near-field EM waves are employed.

In practice, RF-based wireless energy has to be transferred via a signal with high carrier frequency such that antennas with small size can be used for harvesting the power in portable devices. However, the associated path loss severely attenuates the signal leading to a small amount of harvested energy at the receiver. For instance, for the short distance of 10 meters in free space, the attenuation of a wireless signal can be up to 50 dB for a carrier frequency of 915 MHz in the industrial, scientific, and medical radio (ISM) frequency band. Hence, multiple antenna beamforming

has been proposed to improve the efficiency of WPT [11]–[14]. With the spatial degrees of freedom offered by multiple antennas, one can focus information and energy beams which improves the beamforming efficiency for information transfer and WPT. On the other hand, with the existing RF-based hardware circuit technology, the minimum required received power at an information receiver is -60 dBm, while that of an RF-based energy harvesting receiver is -10 dBm. In order to satisfy the sensitivity requirements, an RF-based energy harvesting receiver has to be located closer to the transmitter than an information receiver. Also, the transmitters can increase the energy of the information-carrying signal to facilitate RF energy harvesting at the receivers. However, these two common remedies may also increase the possibility of information leakage to eavesdroppers due to the associated higher signal power. Therefore, new quality of service (QoS) concerns regarding communication security and efficient WPT naturally arise in systems providing SWIPT services [21]–[26].

In fact, security is a crucial problem in wireless communication systems in general due to the broadcast nature of the wireless medium. Traditionally, communication security relies on cryptographic encryption algorithms employed at the application layer. Yet, these algorithms assume perfect secret key management and distribution which may not be possible in future wireless IoT networks with a massive number of wireless sensor nodes. Alternatively, information-theoretic physical layer (PHY) security offers a complementary technology to cryptographic encryption [27]–[33]. The principle of PHY security is to exploit the physical characteristics of the wireless fading channel to ensure perfect secrecy of communication. In particular, it has been shown that in a wire-tap channel, a source and a destination can exchange perfectly secure information if the source-destination channel offers better conditions compared to the source-eavesdropper channel [27]. Hence, multiple-antenna technology has been proposed to ensure secure communication. Specifically, by exploiting the extra degrees of freedom introduced by multiple antennas, artificial noise is injected into the communication channel intentionally to impair the received signals at the eavesdroppers. The notion of communication security for SWIPT systems has recently been pursued in [21, 22]. In particular, the dual use of energy signals for facilitating efficient WPT and providing communication security was proposed. However, the beamforming design for secure SWIPT systems in [21, 22] were based on a linear EH model which does not capture the highly non-linear characteristics of practical end-to-end WPT. In particular, existing beamforming schemes designed for a linear EH model may lead to severe resource allocation mismatches resulting in performance degradation in WPT and secure communications. Hence, in this chapter, we study beamforming designs enabling secure SWIPT based on a non-linear EH model.

The remainder of this chapter is organized as follows. In Section 2, we introduce the adopted channel model and the RF EH model. Section 3 studies the beamforming design for guaranteeing secure communication in SWIPT systems and simulation results are provided in Section 4. In Section 5, we conclude with a brief summary of this chapter.

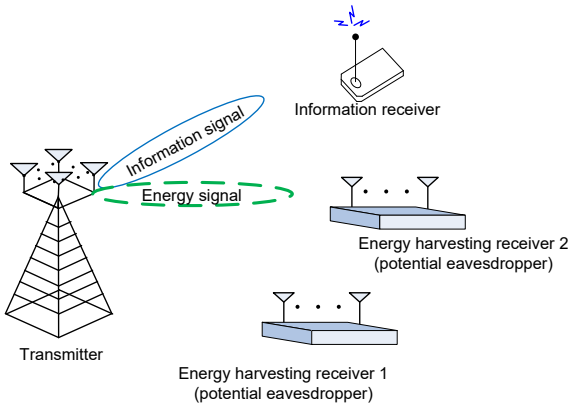

Figure 1: A multiuser SWIPT model with an IR and $J = 2$ ERs. The transmitter emits both an information signal and an energy signal to facilitate secure communication for the IR and efficient WPT.

Notation

We use boldface capital and lower case letters to denote matrices and vectors, respectively. $\mathbf{A}^H$, $\mathrm{Tr}(\mathbf{A})$, $\mathrm{Rank}(\mathbf{A})$, and $\det(\mathbf{A})$ represent the Hermitian transpose, trace, rank, and determinant of matrix $\mathbf{A}$, respectively; $\mathbf{A} \succ \mathbf{0}$ and $\mathbf{A} \succeq \mathbf{0}$ indicate that $\mathbf{A}$ is a positive definite and a positive semidefinite matrix, respectively; $\lambda_{\max}(\mathbf{A})$ denotes the maximum eigenvalue of matrix $\mathbf{A}$; $\mathbf{I}_N$ is the $N \times N$ identity matrix; $\mathbb{C}^{N\times M}$ denotes the set of all $N \times M$ matrices with complex entries; $\mathbb{H}^N$ denotes the set of all $N \times N$ Hermitian matrices. The circularly symmetric complex Gaussian (CSCG) distribution is denoted by $\mathcal{CN}(\mathbf{m}, \mathbf{\Sigma})$ with mean vector $\mathbf{m}$ and covariance matrix $\mathbf{\Sigma}$; $\sim$ indicates "distributed as"; $\mathcal{E}\{\cdot\}$ denotes statistical expectation; $|\cdot|$ represents the absolute value of a complex scalar. $[x]^+$ stands for $\max\{0, x\}$.

2. Channel Model

A downlink frequency flat fading channel is considered. We assume that the SWIPT system comprises a transmitter, an information receiver (IR), and J energy harvesting receivers (ER), cf. Figure 1. The transmitter is equipped with $N_{\mathrm{T}} \geq 1$ antennas. The IR is a single-antenna device and each ER is equipped with $N_{\mathrm{R}} \geq 1$ receive antennas to facilitate energy harvesting. In SWIPT systems, the signals intended for the IR are overheard by the ERs since all receivers are in the range of service coverage. If the ERs are malicious, they may eavesdrop the information signal intended for IR. Hence, the ERs are potential eavesdroppers which should be taken into account for providing secure communication. We assume that $N_{\mathrm{T}} > N_{\mathrm{R}}$ for the study of beamforming design. In each time slot, the received signals at the IR

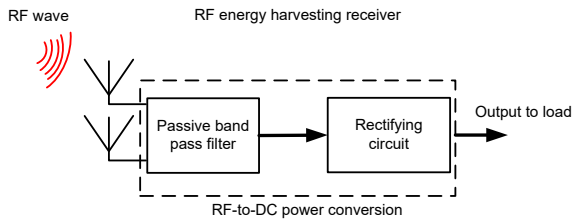

Figure 2: Block diagram of an ER.

and ER $j \in \{1, \ldots, J\}$ are given by

$$y = \mathbf{h}^H(\mathbf{w}s + \mathbf{w}_{\mathrm{E}}) + n \text{ and} \quad (1)$$

$$\mathbf{y}_{\mathrm{ER}_j} = \mathbf{G}_j^H(\mathbf{w}s + \mathbf{w}_{\mathrm{E}}) + \mathbf{n}_{\mathrm{ER}_j},\ \forall j \in \{1, \ldots, J\}, \quad (2)$$

respectively, where $s \in \mathbb{C}$ and $\mathbf{w} \in \mathbb{C}^{N_{\mathrm{T}} \times 1}$ are the data symbol and the information beamforming vector, respectively. Without loss of generality, we assume that $\mathcal{E}\{|s|^2\} = 1$. $\mathbf{w}_{\mathrm{E}} \in \mathbb{C}^{N_{\mathrm{T}} \times 1}$ is an energy signal vector which is a Gaussian pseudo-random sequence generated by the transmitter to facilitate efficient WPT and to guarantee communication security. In particular, $\mathbf{w}_{\mathrm{E}}$ is modeled as a complex Gaussian random vector with

$$\mathbf{w}_{\mathrm{E}} \sim \mathcal{CN}(\mathbf{0}, \mathbf{W}_{\mathrm{E}}), \quad (3)$$

where $\mathbf{W}_{\mathrm{E}} \in \mathbb{H}^{N_{\mathrm{T}}}, \mathbf{W}_{\mathrm{E}} \succeq \mathbf{0}$, denotes the covariance matrix of the pseudo-random energy signal. The channel vector between the transmitter and the IR is denoted by $\mathbf{h} \in \mathbb{C}^{N_{\mathrm{T}} \times 1}$ and the channel matrix between the transmitter and ER j is denoted by $\mathbf{G}_j \in \mathbb{C}^{N_{\mathrm{T}} \times N_{\mathrm{R}}}$. $n \sim \mathcal{CN}(0, \sigma_{\mathrm{s}}^2)$ and $\mathbf{n}_{\mathrm{ER}_j} \sim \mathcal{CN}(\mathbf{0}, \sigma_{\mathrm{s}}^2 \mathbf{I}_{N_{\mathrm{R}}})$ are the additive white Gaussian noises (AWGN) at the IR and ER j, respectively, where σ_{s}^2 denotes the noise power at the receiver.

2.1 Non-linear Energy Harvesting Model

Figure 2 depicts the block diagram of an ER for SWIPT systems. In general, the RF-energy harvesting circuit consists of a bandpass filter and a rectifying circuit which converts the received RF power to direct current (DC) power. The total received RF power at ER j is given by

$$P_{\mathrm{ER}_j} = \mathrm{Tr}\left((\mathbf{w}\mathbf{w}^H + \mathbf{W}_{\mathrm{E}})\mathbf{G}_j\mathbf{G}_j^H\right). \quad (4)$$

In the SWIPT literature [35]–[43], for simplicity, the total harvested power at ER j is typically modelled by a linear equation:

$$\Phi_{\mathrm{ER}_j}^{\mathrm{Linear}} = \eta_j P_{\mathrm{ER}_j}, \quad (5)$$

where $0 \leq \eta_j \leq 1$ is the constant power conversion efficiency of ER j. In other words, the total harvested power at the ER is linearly and directly proportional to

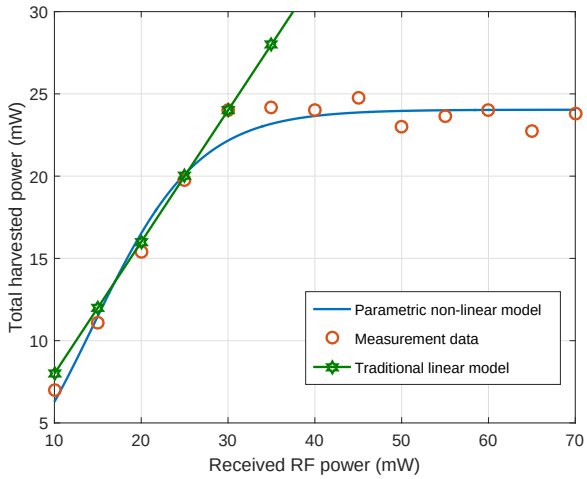

Figure 3: A comparison between experimental data from [34], the harvested power for the non-linear model in (6), and the linear energy harvesting model with $\eta_j = 0.8$ in (5).

the received RF power. Although the linear model leads to simple beamforming designs, it has been shown in recent experiments that practical RF-based energy harvesting circuits [34]–[45] introduce various non-linearities into the end-to-end WPT. In order to design a beamformer for practical secure SWIPT systems, we adopt the non-linear parametric energy harvesting model from [26, 46]. Thus, the total harvested power at ER j, Φ_{ER_j}, is modelled as:

$$\Phi_{\mathrm{ER}_j} = \frac{[\Psi_{\mathrm{ER}_j} - M_j\Omega_j]}{1-\Omega_j}, \; \Omega_j = \frac{1}{1+\exp(a_j b_j)}, \tag{6}$$

$$\text{where } \Psi_{\mathrm{ER}_j} = \frac{M_j}{1+\exp\Big(-a_j(P_{\mathrm{ER}_j} - b_j)\Big)} \tag{7}$$

is a logistic function which has the received RF power, P_{ER_j}, as its input. M_j is a constant denoting the maximum harvested power at ER j when the EH circuit is saturated because of exceedingly large input power. Parameters a_j and b_j are constants which capture the joint effects of resistance, capacitance, and circuit sensitivity. Specifically, a_j reflects the non-linear charging rate with respect to the input power, P_{ER_j}, and b_j is related to the minimum turn-on voltage of the EH circuit. In practice, the parameters a_j, b_j, and M_j of the model in (6) can be easily obtained using standard curve fitting algorithms for a given energy harvesting hardware circuit. In fact, it has been verified by experimental results that the proposed parametric non-linear model is able to accurately capture the dynamics of the RF energy conversion efficiency and the joint effects of the non-linear phenom-

ena caused by hardware imperfections at different input power levels. In Figure 3, we show an example for the curve fitting for the non-linear EH model in (6) with parameters $M_j = 0.024$, $b_j = 0.014$, and $a_j = 150$ for ER j. It can be observed that the parametric non-linear model shows an excellent agreement with the experimental results provided in [34] for the wireless power harvested by a practical EH circuit. Figure 3 also illustrates the inability of the linear model in (5) to capture the non-linear characteristics of practical EH circuits, especially in the high received RF power regime.

2.2 Achievable Secrecy Rate

Assuming perfect CSI at the IR for coherent signal detection, the achievable data rate (bit/s/Hz) between the transmitter and the IR is given by

$$R = \log_2\left(1+\frac{\mathbf{w}^H\mathbf{H}\mathbf{w}}{\sigma_{\mathrm{s}}^2}\right), \tag{8}$$

where $\mathbf{H} = \mathbf{h}\mathbf{h}^H$. We note that since the energy signal is known to both the transmitter and the IR, the interference caused by the energy signal, i.e., $\mathrm{Tr}(\mathbf{H}\mathbf{W}_{\mathrm{E}})$ can be removed at the IR via SIC to improve the data rate.

In order to provide secure communication to the IR, all the ERs are treated as potential eavesdroppers and are taken into account for beamforming design. Besides, we focus on the worst-case scenario. In particular, we assume noiseless ERs. Therefore, the capacity between the transmitter and ER j for decoding the signal of the IR can be expressed as

$$\begin{aligned} R_{\mathrm{ER}_j} &= \log_2\det(\mathbf{I}_{N_{\mathrm{R}}}+\mathbf{Q}_j^{-1}\mathbf{G}_j^H\mathbf{w}\mathbf{w}^H\mathbf{G}_j), \\ \mathbf{Q}_j &= \mathbf{G}_j^H\mathbf{W}_{\mathrm{E}}\mathbf{G}_j \succ \mathbf{0}, \end{aligned} \tag{9}$$

where $\mathbf{Q}_j$ is the interference covariance matrix for ER j assuming the worst case for communication secrecy. We note that in contrast to the IR, the energy signal is not known to the ERs and appears random to them. Hence, the energy signal cannot be removed via interference cancellation techniques at the ERs. Thus, the achievable secrecy rate of the IR is given by [30, 33]

$$R_{\mathrm{sec}} = \left[R-\max_{\forall j}\left\{R_{\mathrm{ER}_j}\right\}\right]^+. \tag{10}$$

3. Problem Formulation and Solution

The considered system design objective is to maximize the secrecy rate at the IR while guaranteeing a minimum harvested power at each ER. The beamforming design is formulated as the following optimization problem:

Problem 1. Resource Allocation for Secrecy Rate Maximization

$$\begin{aligned} \underset{\mathbf{W}_{\mathrm{E}}\in\mathbb{H}^{N_{\mathrm{T}}},\mathbf{w}}{\text{maximize}} \quad & \log_2\left(1+\frac{\mathbf{w}^H\mathbf{H}\mathbf{w}}{\sigma_{\mathrm{s}}^2}\right)-\max_{\forall j}\left\{R_{\mathrm{ER}_j}\right\} \\ \text{subject to} \quad & \mathrm{C1}:\ \|\mathbf{w}\|_2^2+\mathrm{Tr}(\mathbf{W}_{\mathrm{E}})\le P_{\max}, \\ & \mathrm{C2}:\ \Phi_{\mathrm{ER}_j}\ge P_{\mathrm{req}_j}^{\min},\forall j\in\{1,\ldots,J\}, \\ & \mathrm{C3}:\ \mathbf{W}_{\mathrm{E}}\succeq\mathbf{0}\,. \end{aligned} \tag{11}$$

Constants $P_{\max}$ and $P_{\mathrm{req}_j}^{\min}$ in constraints C1 and C2 are the maximum transmit power allowance and the minimum required harvested power at ER j, respectively. Constraint C3 and $\mathbf{W}_{\mathrm{E}}\in\mathbb{H}^{N_{\mathrm{T}}}$ constrain matrix $\mathbf{W}_{\mathrm{E}}$ to be a positive semidefinite Hermitian matrix. We note that the objective function in (11) is equivalent to the achievable secrecy rate of the IR defined in (10), even though the $[\cdot]^+$ operator has been removed. This is because if the problem is feasible, the optimal beamforming design can always set $\mathbf{w}=\mathbf{0}$ to ensure a non-negative secrecy rate.

The objective function in (11) is a non-convex function due to the difference of two logarithmic functions. In particular, the log-det function in R_{ER_j} of the subtrahend of the objective function is non-convex. In order to obtain a globally optimal solution, we introduce several transformations in (11) in the following.

Optimization Problem Solution

In order to handle the non-convex objective function, we first introduce an auxiliary optimization variable τ and rewrite optimization problem (11) in the following equivalent form[1]:

Problem 2. Equivalent Optimization Problem

$$\begin{aligned} \underset{\mathbf{W}_{\mathrm{E}}\in\mathbb{H}^{N_{\mathrm{T}}},\mathbf{w},\tau}{\text{maximize}} \quad & \log_2\left(1+\frac{\mathbf{w}^H\mathbf{H}\mathbf{w}}{\sigma_{\mathrm{s}}^2}\right)-\tau \\ \text{subject to} \quad & \mathrm{C1},\mathrm{C2},\mathrm{C3}, \\ & \mathrm{C4}:\ \tau\ge\log_2\det(\mathbf{I}_{N_{\mathrm{R}}}+\mathbf{Q}_j^{-1}\mathbf{G}_j^H\mathbf{w}\mathbf{w}^H\mathbf{G}_j),\forall j. \end{aligned} \tag{12}$$

We note that the objective function of the transformed problem is now jointly concave with respect to the optimization variables. Nevertheless, the new constraint C4 is non-convex. Hence, we solve the optimization problem in (12) for a fixed τ and obtain the corresponding beamforming design. Then, by adopting a one-

[1] In this chapter, "equivalent" means that both problem formulations lead to the same beamforming design.

dimensional search, we find the optimal value of the optimization problem and the corresponding τ[2].

Therefore, in the sequel, we focus on solving Problem 2 for a given τ. First, we further transform the considered problem into the following equivalent form:

Problem 3. Rank-constrained Optimization Problem

$$\begin{aligned}
\underset{\mathbf{W}_{\mathrm{E}}\in\mathbb{H}^{N_{\mathrm{T}}},\mathbf{W},\beta_j,\delta}{\text{maximize}} \quad & \log_2\left(1+\frac{\delta}{\sigma_{\mathrm{s}}^2}\right)-\tau \qquad (13)\\
\text{subject to} \quad & \mathrm{C1}:\ \mathrm{Tr}(\mathbf{W})+\mathrm{Tr}(\mathbf{W}_{\mathrm{E}})\le P_{\max},\\
& \mathrm{C2}:\ \frac{M_j}{1+\exp\Big(-a_j(\beta_j-b_j)\Big)}\ge P_{\mathrm{req}_j}^{\min}(1-\Omega_j)+M_j\Omega_j,\forall j,\\
& \mathrm{C3}:\ \mathbf{W}_{\mathrm{E}}\succeq\mathbf{0},\\
& \mathrm{C4}:\ \tau\ge\log_2\det(\mathbf{I}_{N_{\mathrm{R}}}+\mathbf{Q}_j^{-1}\mathbf{G}_j^H\mathbf{W}\mathbf{G}_j),\forall j,\\
& \mathrm{C5}:\ \delta\le\mathrm{Tr}(\mathbf{H}\mathbf{W}),\\
& \mathrm{C6}:\ \beta_j\le\mathrm{Tr}\Big((\mathbf{W}+\mathbf{W}_{\mathrm{E}})\mathbf{G}_j\mathbf{G}_j^H\Big),\forall j,\\
& \mathrm{C7}:\ \mathrm{Rank}(\mathbf{W})\le 1,\\
& \mathrm{C8}:\ \mathbf{W}\succeq\mathbf{0},
\end{aligned}$$

where $\mathbf{W}=\mathbf{w}\mathbf{w}^H$ is a new optimization variable matrix. Auxiliary optimization variables β_j and δ are introduced to simplify the analysis of the solution in the following. It can be observed that the non-convexity of the transformed problem arises from the log-det function in C4 and the combinatorial rank constraint C7. To circumvent the non-convexity, we first introduce the following proposition to handle constraint C4. Then, we handle the rank constraint C7 by recasting the considered problem as a convex optimization problem via SDP relaxation.

Proposition 1. *For $\tau>0$, the following implication holds for constraint C4:*

$$\mathrm{C4}\Rightarrow\overline{\mathrm{C4}}\text{:}\ \mathbf{G}_j^H\mathbf{W}\mathbf{G}_j\ \preceq\ \alpha_{\mathrm{ER}}\mathbf{Q}_j,\ \forall j, \qquad (14)$$

where $\alpha_{\mathrm{ER}}=2^{\tau}-1$ is an auxiliary constant and $\overline{C4}$ is an linear matrix inequality (LMI) constraint. We note that constraints $\overline{C4}$ and C4 are equivalent, i.e., $\overline{C4}\Leftrightarrow C4$, when $\mathrm{Rank}(\mathbf{W})\le 1$.

Proof: Please refer to Appendix 6.1 for the proof. ■

[2]We note that the range of τ is $0\le\tau\le\tau_{\max}$, where $\tau_{\max}$ can be found by solving (13) with the right hand side of constraint C4 set as zero.

Now, we apply Proposition 1 to Problem 3 by replacing constraint C4 with constraint $\overline{\text{C4}}$. Then, we adopt SDP relaxation [47] by removing constraint C7 which yields

Problem 4. Semidefinite Relaxation of Problem 3

$$
\begin{aligned}
\underset{\mathbf{W}_{\mathrm{E}}\in\mathbb{H}^{N_{\mathrm{T}}},\mathbf{W},\beta_j,\delta}{\text{maximize}} \quad & \log_2\left(1+\frac{\delta}{\sigma_{\mathrm{s}}^2}\right)-\tau && (15)\\
\text{subject to} \quad & \text{C1}: \ \mathrm{Tr}(\mathbf{W})+\mathrm{Tr}(\mathbf{W}_{\mathrm{E}})\leq P_{\max},\\
& \text{C2}: \ \frac{M_j}{1+\exp\Big(-a_j(\beta_j-b_j)\Big)}\geq P_{\mathrm{req}_j}^{\min}(1-\Omega_j)+M_j\Omega_j, \forall j,\\
& \text{C3}: \ \mathbf{W}_{\mathrm{E}}\succeq\mathbf{0},\\
& \overline{\text{C4}}: \ \mathbf{G}_j^H\mathbf{W}\mathbf{G}_j\preceq\alpha_{\mathrm{ER}}\mathbf{G}_j^H\mathbf{W}_{\mathrm{E}}\mathbf{G}_j, \ \forall j,\\
& \text{C5}: \ \delta\leq\mathrm{Tr}(\mathbf{H}\mathbf{W}),\\
& \text{C6}: \ \beta_j\leq\mathrm{Tr}\Big((\mathbf{W}+\mathbf{W}_{\mathrm{E}})\mathbf{G}_j\mathbf{G}_j^H\Big), \forall j\\
& \text{C7}: \ \cancel{\mathrm{Rank}(\mathbf{W})\leq 1},\\
& \text{C8}: \ \mathbf{W}\succeq\mathbf{0}\,.
\end{aligned}
$$

As a result, the relaxed problem becomes a standard convex optimization problem and can be solved efficiently by numerical solvers such as CVX [48] via the interior point method. However, the relaxation may not be tight if $\mathrm{Rank}(\mathbf{W})>1$ occurs. Therefore, we reveal the tightness of the adopted SDP relaxation in (11) in the following theorem.

Theorem 1. *Let the optimal beamforming matrix and energy covariance matrix of* (15) *be* $\mathbf{W}^*$ *and* $\mathbf{W}_{\mathrm{E}}^*$*, respectively. Assuming the considered problem is feasible for* $P_{\max}>0$*, then* $\mathrm{Rank}(\mathbf{W}^*)\leq 1, \forall k$*, and* $\mathrm{Rank}(\mathbf{W}_{\mathrm{E}}^*)\leq 1$*.*

Proof: Please refer to Appendix 6.2. ■

In other words, (11) can be solved optimally. Hence, information beamforming and energy beamforming are optimal for the maximization of the secrecy rate, despite the non-linearity of the EH circuit.

4. Results

In this section, we evaluate the system performance of the proposed optimal resource allocation algorithm via simulations. We summarize the relevant simulation parameters in Table 1. We assume that the IR and the ERs are located 100 meters and 5 meters from the transmitter, respectively. For the non-linear EH circuits, we set $M_j=24$ mW which corresponds to the maximum harvested power per ER. Besides, we adopt $a_j=150$ and $b_j=0.0014$. For the optimal beamforming design,

Table 1: Simulation Parameters

Carrier center frequency	915 MHz
Bandwidth	200 kHz
Transceiver antenna gain	10 dBi
Noise power σ^2	-95 dBm
Min. harvested power at each ER $P_{\text{req}_j}^{\min}$	3 dBm
Transmitter-to-ER fading distribution	Rician with Rician factor 3 dB
Transmitter-to-IR fading distribution	Rayleigh

we use 100 equally spaced intervals for quantizing the range of τ for facilitating the one-dimensional search. We solve the optimization problem in (2) and obtain the average system performance by averaging over different channel realizations. We note that the considered problem may be infeasible when the QoS requirements are stringent and/or the channels are in unfavourable conditions. In the simulation, we set the secrecy rate of the corresponding channel realizations to zero to account for the penalty incurred by an infeasible problem.

In Figure 4, we study the average secrecy rate versus the maximum transmit power at the transmitter, $P_{\max}$, for different numbers of transmit antennas and beamforming schemes. As can be observed, the average secrecy rate increases with $P_{\max}$. Indeed, with more available transmit power, the transmitter is able to increase the signal strength of the information signal. Besides, a higher power can also be allocated to the energy signal to degrade the channel quality of the ERs for information decoding. On the other hand, it can be seen that the achievable secrecy rate improves with the number of transmit antennas. In fact, the spatial degrees of freedom offered by extra transmit antennas facilitate a more flexible beamforming. In particular, the transmitter can steer the energy signal and the information signal towards the ERs more accurately to improve the efficiency of WPT. For comparison, we also show the performance of two baseline schemes. For baseline scheme 1, the beamforming is designed for the non-linear EH model in (6). However, the power of the energy signal is set to zero and we solve the corresponding beamforming design problem in (15). For baseline 2, the existing linear EH model with $\eta_j = 1$, cf. (5), is adopted for beamforming design. Based on the linear EH model and assuming that at most half of the power is allocated to the information signal, we optimize $\mathbf{w}$ and $\mathbf{W}_{\text{E}}$ to maximize the secrecy rate subject to the constraints in (11). It can be observed that the proposed optimal algorithm designed for the non-linear energy harvesting model provides a substantial performance gain compared to the two baseline schemes. In particular, baseline 1 obtains the worst system performance among all the schemes. In fact, transmitting an energy signal is necessary for achieving a high secrecy rate in SWIPT. On the other hand, although baseline scheme 2 also employs an energy signal, baseline scheme 2 may suffer from severe mismatches in resource allocation since it does not account for the non-linear nature of the energy harvesting circuits.

Figure 5 shows the average secrecy rate versus the number of ERs for different beamforming schemes and different numbers of receive antennas equipped at each

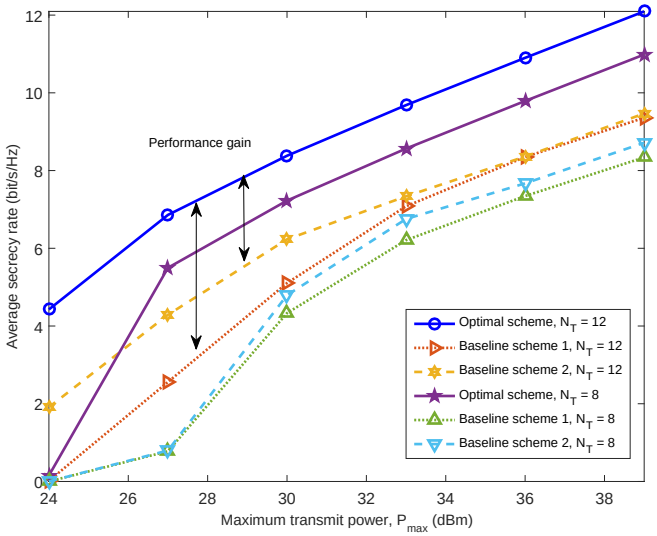

Figure 4: Average secrecy rate (bit/s/Hz) versus the maximum available transmit power (dBm). There are $N_{\mathrm{R}} = 3$ antennas equipped at each ER. The double sided arrows represent the performance gains due to the proposed optimization.

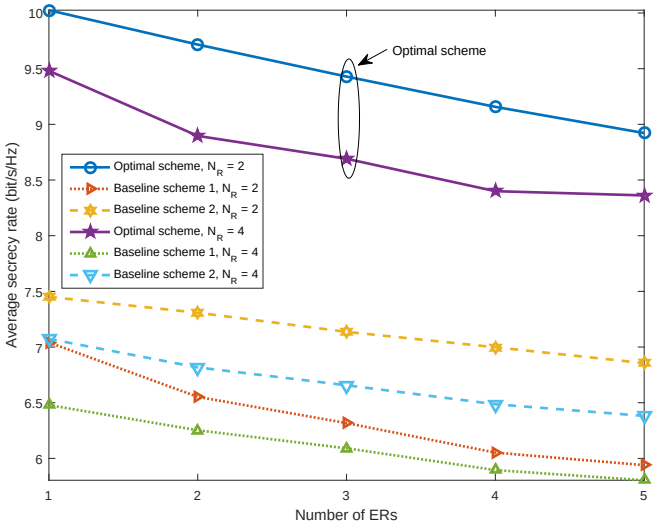

Figure 5: Average system secrecy rate (bit/s/Hz) versus the number of ERs. There are $N_{\mathrm{T}} = 8$ antennas equipped at the transmitter.

ER. The maximum transmit power at the transmitter is $P_{\max} = 33$ dBm. It can be observed that the average system secrecy rate, i.e., R_{sec}, is a non-increasing function with respect to the number of ERs for the following two reasons. First, the minimum required harvested power constraint in C2 becomes more stringent when more ERs are in the system. In particular, the transmitter is forced to focus some of the energy of the information signal towards the ERs in order to satisfy the constraints. Second, there are more potential eavesdroppers present in the system resulting in a higher potential for information leakage. Thus, a higher amount of transmit power has to be allocated to the energy signal for interfering the ERs to guarantee communication secrecy. Hence, less power can be allocated to the desired signal. Also, it can be observed that the average secrecy rate decreases with the number of antennas equipped at each ER, N_{R}. In fact, the signal reception capability of the ERs improves with N_{R}. On the one hand, the ERs can harvest the wireless energy more efficiently which makes constraint C2 less stringent. However, on the other hand, it also makes the considered system more vulnerable to eavesdropping. Therefore, there is a non-trivial tradeoff between the secrecy rate and the number of receive antennas equipped at ERs in the considered system. We also compare the performance of the proposed optimal beamforming scheme with the two baseline schemes. As expected, the optimal scheme outperforms the baseline schemes. This is because the proposed optimal scheme is able to fully exploit the available degrees of freedom for efficient beamforming design.

5. Conclusions

In this chapter, beamforming design for secure SWIPT was studied which is of fundamental importance for wireless sensor networks facilitating IoT. The design was formulated as a non-convex optimization problem for the maximization of the secrecy rate of the information receiver. The problem formulation took into account a minimum required power transfer to practical non-linear ERs. The optimization problem was solved by a one-dimensional search and SDP relaxation. Numerical results showed the potential gains in secrecy rate enabled by the proposed optimization.

Acknowledgements

This work was supported in part by the AvH Professorship Program of the Alexander von Humboldt Foundation. D. W. K. Ng is supported under the Australian Research Council's Discovery Early Career Researcher Award funding scheme (project number DE170100137).

6. Appendix

6.1 Proof of Proposition 1

We start the proof by rewriting constraint C4 as

$$\text{C4: } \log_2 \det(\mathbf{I}_{N_\mathrm{R}} + \mathbf{Q}_j^{-1}\mathbf{G}_j^H\mathbf{W}\mathbf{G}_j) \leq \tau \tag{16}$$

$$\iff \det(\mathbf{I}_{N_\mathrm{R}} + \mathbf{Q}_j^{-1/2}\mathbf{G}_j^H\mathbf{W}\mathbf{G}_j\mathbf{Q}_j^{-1/2}) \leq 1 + \alpha_{\mathrm{ER}}. \tag{17}$$

Then, we propose a lower bound on the left hand side of (17) by introducing the following lemma.

Lemma 1. *For any square matrix $\mathbf{A} \succeq \mathbf{0}$, we have the following inequality [49]:*

$$\det(\mathbf{I} + \mathbf{A}) \geq 1 + \mathrm{Tr}(\mathbf{A}), \tag{18}$$

where the equality holds if and only if $\mathrm{Rank}(\mathbf{A}) \leq 1$.

Exploiting Lemma 1, the left hand side of (17) is bounded below by

$$\begin{aligned} & \det(\mathbf{I}_{N_\mathrm{R}} + \mathbf{Q}_j^{-1/2}\mathbf{G}_j^H\mathbf{W}\mathbf{G}_j\mathbf{Q}_j^{-1/2}) \\ \geq \;& 1 + \mathrm{Tr}(\mathbf{Q}_j^{-1/2}\mathbf{G}_j^H\mathbf{W}\mathbf{G}_j\mathbf{Q}_j^{-1/2}). \end{aligned} \tag{19}$$

Subsequently, by combining equations (16), (17), and (19), we have the following implications:

$$\begin{aligned} & (16) \iff (17) \\ \implies & \mathrm{Tr}(\mathbf{Q}_j^{-1/2}\mathbf{G}_j^H\mathbf{W}\mathbf{G}_j\mathbf{Q}_j^{-1/2}) \leq \alpha_{\mathrm{ER}} && \text{(20a)} \\ \implies & \lambda_{\max}(\mathbf{Q}_j^{-1/2}\mathbf{G}_j^H\mathbf{W}\mathbf{G}_j\mathbf{Q}_j^{-1/2}) \leq \alpha_{\mathrm{ER}} && \text{(20b)} \\ \iff & \mathbf{Q}_j^{-1/2}\mathbf{G}_j^H\mathbf{W}\mathbf{G}_j\mathbf{Q}_j^{-1/2} \preceq \alpha_{\mathrm{ER}}\mathbf{I}_{N_\mathrm{R}} && \text{(20c)} \\ \iff & \mathbf{G}_j^H\mathbf{W}\mathbf{G}_j \preceq \alpha_{\mathrm{ER}}\mathbf{Q}_j. && \text{(20d)} \end{aligned}$$

We note that equations (16) and (20d) are equivalent, i.e., C4 $\Leftrightarrow$ $\overline{\text{C4}}$, when $\mathrm{Rank}(\mathbf{W}) \leq 1$. ■

6.2 Proof of Theorem 1

We follow a similar approach as in [47] to prove Theorem 1. We note that Problem 4 is jointly convex with respect to the optimization variables. Besides, it can be verified that the problem satisfies Slater's constraint qualification and thus has zero duality gap. Therefore, to reveal the structure of $\mathbf{W}$ and $\mathbf{W}_\mathrm{E}$, we consider the

Lagrangian of Problem 4 which is given by:

$$\begin{aligned} L = &-\lambda\Big(\operatorname{Tr}(\mathbf{W}) + \operatorname{Tr}(\mathbf{W}_{\mathrm{E}}) - P_{\max}\Big) - \psi(\delta - \operatorname{Tr}(\mathbf{HW})) \\ &- \sum_{j=1}^{J} \theta_j \left(\beta_j - \operatorname{Tr}\left((\mathbf{W}+\mathbf{W}_{\mathrm{E}})\mathbf{G}_j\mathbf{G}_j^H\right)\right) + \operatorname{Tr}(\mathbf{WY}) \\ &+ \sum_{j=1}^{J} \operatorname{Tr}\left(\mathbf{G}_j^H(\alpha_{\mathrm{ER}}\mathbf{W}_{\mathrm{E}} - \mathbf{W})\mathbf{G}_j\mathbf{D}_{\overline{\mathrm{C4}_j}}\right) + \operatorname{Tr}(\mathbf{W}_{\mathrm{E}}\mathbf{Z}) + \boldsymbol{\Delta}, \end{aligned} \tag{21}$$

where $\lambda \geq 0$, $\mathbf{Z} \succeq \mathbf{0}$, $\mathbf{D}_{\overline{\mathrm{C4}_j}} \succeq \mathbf{0}, \forall j \in \{1,\ldots,J\}$, $\psi \geq 0$, $\theta_j \geq 0$, and $\mathbf{Y} \succeq \mathbf{0}$ are the dual variables for constraints C1, C3, C4, C5, C6, and C8, respectively. Besides, $\boldsymbol{\Delta}$ is a collection of variables and constants that are not relevant to the proof. For notational convenience, we denote the optimal primal and dual variables of the SDP relaxed version in (13) by the corresponding variables with an asterisk superscript in the following. Now, we focus on those Karush-Kuhn-Tucker (KKT) conditions which are needed for the proof:

$$\mathbf{Y}^*, \mathbf{Z}^*, \mathbf{D}^*_{\overline{\mathrm{C4}_j}} \succeq \mathbf{0}, \quad \lambda^*, \psi^*, \theta_j^* \geq 0, \tag{22a}$$

$$\mathbf{Y}^*\mathbf{W}^* = \mathbf{0}, \quad \mathbf{Z}^*\mathbf{W}^*_{\mathrm{E}} = \mathbf{0}, \tag{22b}$$

$$\mathbf{Y}^* = \lambda^*\mathbf{I}_{N_{\mathrm{T}}} - \boldsymbol{\Xi}, \tag{22c}$$

$$\boldsymbol{\Xi} = \psi_j\mathbf{H} + \sum_{j=1}^{J} \theta_j^*\mathbf{G}_j\mathbf{G}_j^H - \sum_{j=1}^{J} \mathbf{G}_j\mathbf{D}^*_{\overline{\mathrm{C4}_j}}\mathbf{G}_j^H \tag{22d}$$

$$\mathbf{Z}^* = \lambda^*\mathbf{I}_{N_{\mathrm{T}}} - \sum_{j=1}^{J} \theta_j^*\mathbf{G}_j\mathbf{G}_j^H - \sum_{j=1}^{J} \mathbf{G}_j\mathbf{D}^*_{\overline{\mathrm{C4}_j}}\mathbf{G}_j^H\alpha_{\mathrm{ER}}. \tag{22e}$$

From (22b), we know that the columns of $\mathbf{W}^*$ lie in the null space of $\mathbf{Y}^*$. In order to reveal the rank of $\mathbf{W}^*$, we investigate the structure of $\mathbf{Y}^*$. First, it can be shown that $\lambda^* > 0$ since constraint C1 is active for the optimal solution. Then, we show that $\operatorname{Rank}(\mathbf{W}) \leq 1$ in the following two cases. For the first case, if $\boldsymbol{\Xi}$ is a negative definite matrix, then from (22c), $\mathbf{Y}^*$ becomes a full-rank and positive definite matrix. By (22b), $\mathbf{W}^*$ is forced to be the zero matrix with $\operatorname{Rank}(\mathbf{W}^*) = 0$. For the second case, we focus on $\boldsymbol{\Xi} \succeq \mathbf{0}$. Since matrix $\mathbf{Y}^* = \lambda^*\mathbf{I}_{N_{\mathrm{T}}} - \boldsymbol{\Xi}$ is positive semidefinite, the following inequality holds:

$$\lambda^* \geq \lambda_{\boldsymbol{\Xi}}^{\max} \quad \geq \quad 0, \tag{23}$$

where $\lambda_{\boldsymbol{\Xi}}^{\max}$ is the maximum eigenvalue of matrix $\boldsymbol{\Xi}$. From (22c), if $\lambda^* > \lambda_{\boldsymbol{\Xi}}^{\max}$, matrix $\mathbf{Y}^*$ will become a positive definite matrix with full rank. This will again yield the zero solution, $\mathbf{W}^* = \mathbf{0}$, with $\operatorname{Rank}(\mathbf{W}^*) = 0$. On the other hand, if $\lambda^* = \lambda_{\boldsymbol{\Xi}}^{\max}$, then, in order to have a bounded optimal dual solution, it follows that the null space of $\mathbf{Y}^*$ is spanned by vector $\mathbf{u}_{\boldsymbol{\Xi},\max} \in \mathbb{C}^{N_{\mathrm{T}}\times 1}$, which is the unit-norm eigenvector of $\boldsymbol{\Xi}$ associated with eigenvalue $\lambda_{\boldsymbol{\Xi}}^{\max}$. As a result, the optimal

beamforming matrix $\mathbf{W}^*$ has to be a rank-one matrix and is given by

$$\mathbf{W}^* = \upsilon \mathbf{u}_{\mathbf{\Xi},\max} \mathbf{u}_{\mathbf{\Xi},\max}^H, \tag{24}$$

where υ is a parameter such that the power consumption satisfies constraint C1.

On the other hand, for revealing the structure of $\mathbf{Z}^*$, we focus on (22e). Define an auxiliary variable matrix $\mathbf{B} = \sum_{j=1}^{J} \theta_j \mathbf{G}_j \mathbf{G}_j^H + \sum_{j=1}^{J} \mathbf{G}_j \mathbf{D}_{\overline{\mathrm{C4}_j}} \mathbf{G}_j^H \alpha_{\mathrm{ER}} \succeq \mathbf{0}$ and the corresponding maximum eigenvalue as $\lambda_{\mathbf{B}}^{\max}$. Since $\mathbf{Z}^* \succeq \mathbf{0}$, we have $\lambda^* \geq \lambda_{\mathbf{B}}^{\max} \geq 0$. If $\lambda^* = \lambda_{\mathbf{B}}^{\max}$, then $\mathrm{Rank}(\mathbf{Z}^*) = N_{\mathrm{T}} - 1$ and $\mathrm{Rank}(\mathbf{W}_{\mathrm{E}}^*) = 1$. If $\lambda^* > \lambda_{\mathbf{B}}^{\max}$, then $\mathrm{Rank}(\mathbf{Z}^*) = N_{\mathrm{T}}$ and $\mathrm{Rank}(\mathbf{W}_{\mathrm{E}}^*) = 0$. Therefore, $\mathrm{Rank}(\mathbf{W}_{\mathrm{E}}^*) \leq 1$ and at most one energy beam is required to achieve optimality. ■

Bibliography

[1] M. Zorzi, A. Gluhak, S. Lange, and A. Bassi, "From today's INTRAnet of things to a Future INTERnet of Things: a Wireless- and Mobility-Related View," *IEEE Wireless Commun.*, vol. 17, pp. 44–51, Dec. 2010.

[2] D. W. K. Ng, E. S. Lo, and R. Schober, "Energy-Efficient Resource Allocation in Multi-Cell OFDMA Systems with Limited Backhaul Capacity," *IEEE Trans. Wireless Commun.*, vol. 11, pp. 3618–3631, Oct. 2012.

[3] D. W. K. Ng, Y. Wu, and R. Schober, "Power Efficient Resource Allocation for Full-Duplex Radio Distributed Antenna Networks," *IEEE Trans. Wireless Commun.*, vol. 15, no. 4, pp. 2896–2911, Apr. 2016.

[4] D. W. K. Ng, E. S. Lo, and R. Schober, "Energy-Efficient Resource Allocation in OFDMA Systems with Hybrid Energy Harvesting Base Station," *IEEE Trans. Wireless Commun.*, vol. 12, pp. 3412–3427, Jul. 2013.

[5] I. Ahmed, A. Ikhlef, D. W. K. Ng, and R. Schober, "Power Allocation for an Energy Harvesting Transmitter with Hybrid Energy Sources," *IEEE Trans. Wireless Commun.*, vol. 12, pp. 6255–6267, Dec. 2013.

[6] V. W. S. Wong, R. Schober, D. W. K. Ng, and L.-C. Wang, *Key Technologies for 5G Wireless Systems,* Cambridge University Press, Mar. 2017.

[7] Q. Wu, G. Y. Li, W. Chen, D. W. K. Ng, and R. Schober, "An Overview of Sustainable Green 5G Networks," *accepted for publication, IEEE Wireless Commun.*, Mar. 2017.

[8] I. Hammerstrom and A. Wittneben, "Power Allocation Schemes for Amplify-and-Forward MIMO-OFDM Relay Links," vol. 6, pp. 2798–2802, Aug. 2007.

[9] D. W. K. Ng, E. S. Lo, and R. Schober, "Dynamic Resource Allocation in MIMO-OFDMA Systems with Full-Duplex and Hybrid Relaying," *IEEE Trans. Commun.*, vol. 60, pp. 1291–1304, May 2012.

[10] P. Grover and A. Sahai, "Shannon Meets Tesla: Wireless Information and Power Transfer," in *Proc. IEEE Intern. Sympos. on Inf. Theory*, Jun. 2010, pp. 2363 –2367.

[11] I. Krikidis, S. Timotheou, S. Nikolaou, G. Zheng, D. W. K. Ng, and R. Schober, "Simultaneous Wireless Information and Power Transfer in Modern Communication Systems," *IEEE Commun. Mag.*, vol. 52, no. 11, pp. 104–110, Nov. 2014.

[12] Z. Ding, C. Zhong, D. W. K. Ng, M. Peng, H. A. Suraweera, R. Schober, and H. V. Poor, "Application of Smart Antenna Technologies in Simultaneous Wireless Information and Power Transfer," *IEEE Commun. Mag.*, vol. 53, no. 4, pp. 86–93, Apr. 2015.

[13] X. Chen, Z. Zhang, H.-H. Chen, and H. Zhang, "Enhancing Wireless Information and Power Transfer by Exploiting Multi-Antenna Techniques," *IEEE Commun. Mag.*, no. 4, pp. 133–141, Apr. 2015.

[14] X. Chen, D. W. K. Ng, and H.-H. Chen, "Secrecy Wireless Information and Power Transfer: Challenges and Opportunities," *IEEE Commun. Mag.*, 2016.

[15] Q. Wu, M. Tao, D. Ng, W. Chen, and R. Schober, "Energy-Efficient Resource Allocation for Wireless Powered Communication Networks," *IEEE Trans. Wireless Commun.*, vol. 15, pp. 2312–2327, Mar. 2016.

[16] Q. Wu, W. Chen, D. W. K. Ng, J. Li, and R. Schober, "User-Centric Energy Efficiency Maximization for Wireless Powered Communications," *IEEE Trans. Wireless Commun.*, vol. 15, no. 10, pp. 6898–6912, Oct. 2016.

[17] X. Chen, X. Wang, and X. Chen, "Energy-Efficient Optimization for Wireless Information and Power Transfer in Large-Scale MIMO Systems Employing Energy Beamforming," *IEEE Wireless Commun. Lett.*, vol. 2, pp. 1–4, Dec. 2013.

[18] D. W. K. Ng, E. S. Lo, and R. Schober, "Wireless Information and Power Transfer: Energy Efficiency Optimization in OFDMA Systems," *IEEE Trans. Wireless Commun.*, vol. 12, pp. 6352–6370, Dec. 2013.

[19] R. Zhang and C. K. Ho, "MIMO Broadcasting for Simultaneous Wireless Information and Power Transfer," *IEEE Trans. Wireless Commun.*, vol. 12, pp. 1989–2001, May 2013.

[20] S. Leng, D. W. K. Ng, N. Zlatanov, and R. Schober, "Multi-Objective Resource Allocation in Full-Duplex SWIPT Systems," in *Proc. IEEE Intern. Commun. Conf.*, 2016.

[21] D. W. K. Ng, E. S. Lo, and R. Schober, "Robust Beamforming for Secure Communication in Systems with Wireless Information and Power Transfer," *IEEE Trans. Wireless Commun.*, vol. 13, pp. 4599–4615, Aug. 2014.

[22] D. W. K. Ng and R. Schober, "Secure and Green SWIPT in Distributed Antenna Networks with Limited Backhaul Capacity," *IEEE Trans. Wireless Commun.*, vol. 14, no. 9, pp. 5082–5097, Sep. 2015.

[23] M. Khandaker and K.-K. Wong, "Robust Secrecy Beamforming With Energy-Harvesting Eavesdroppers," *IEEE Wireless Commun. Lett.*, vol. 4, pp. 10–13, Feb. 2015.

[24] Q. Wu, W. Chen, and J. Li, "Wireless Powered Communications With Initial Energy: QoS Guaranteed Energy-Efficient Resource Allocation," *IEEE Wireless Commun. Lett.*, vol. 19, Dec. 2015.

[25] N. Zlatanov, Z. Hadzi-Velkov, and D. W. K. Ng, *Asymptotically Optimal Power Allocation for Wireless Powered Communication Network with Non-orthogonal Multiple Access.* Springer International Publishing, 2016. [Online]. Available: http://dx.doi.org/10.1007/978-3-319-46810-5_10

[26] E. Boshkovska, D. Ng, N. Zlatanov, and R. Schober, "Practical Non-Linear Energy Harvesting Model and Resource Allocation for SWIPT Systems," *IEEE Commun. Lett.*, vol. 19, pp. 2082–2085, Dec. 2015.

[27] A. D. Wyner, "The Wire-Tap Channel," Tech. Rep., Oct. 1975.

[28] X. Chen, D. W. K. Ng, W. Gerstacker, and H. H. Chen, "A Survey on Multiple-Antenna Techniques for Physical Layer Security," *IEEE Commun. Surveys Tuts.*, vol. PP, no. 99, pp. 1–1, 2016.

[29] J. Zhu, R. Schober, and V. Bhargava, "Secure Transmission in Multicell Massive MIMO Systems," *IEEE Trans. Wireless Commun.*, vol. 13, pp. 4766–4781, Sep. 2014.

[30] S. Goel and R. Negi, "Guaranteeing Secrecy using Artificial Noise," *IEEE Trans. Wireless Commun.*, vol. 7, pp. 2180 – 2189, Jun. 2008.

[31] H. M. Wang, C. Wang, D. Ng, M. Lee, and J. Xiao, "Artificial Noise Assisted Secure Transmission for Distributed Antenna Systems," *IEEE Trans. Signal Process.*, vol. PP, no. 99, pp. 1–1, 2016.

[32] J. Chen, X. Chen, W. H. Gerstacker, and D. W. K. Ng, "Resource Allocation for a Massive MIMO Relay Aided Secure Communication," *IEEE Trans. on Inf. Forensics and Security*, vol. 11, no. 8, pp. 1700–1711, Aug. 2016.

[33] D. W. K. Ng, E. S. Lo, and R. Schober, "Efficient Resource Allocation for Secure OFDMA Systems," *IEEE Trans. Veh. Technol.*, vol. 61, pp. 2572–2585, Jul. 2012.

[34] J. Guo and X. Zhu, "An Improved Analytical Model for RF-DC Conversion Efficiency in Microwave Rectifiers," in *IEEE MTT-S Int. Microw. Symp. Dig.*, Jun. 2012, pp. 1–3.

[35] X. Zhou, R. Zhang, and C. K. Ho, "Wireless Information and Power Transfer: Architecture Design and Rate-Energy Tradeoff," in *Proc. IEEE Global Telecommun. Conf.*, Dec. 2012.

[36] D. W. K. Ng, E. S. Lo, and R. Schober, "Energy-Efficient Resource Allocation in Multiuser OFDM Systems with Wireless Information and Power Transfer," in *Proc. IEEE Wireless Commun. and Netw. Conf.*, 2013.

[37] S. Leng, D. W. K. Ng, and R. Schober, "Power Efficient and Secure Multiuser Communication Systems with Wireless Information and Power Transfer," in *Proc. IEEE Intern. Commun. Conf.*, Jun. 2014.

[38] D. W. K. Ng, L. Xiang, and R. Schober, "Multi-Objective Beamforming for Secure Communication in Systems with Wireless Information and Power Transfer," in *Proc. IEEE Personal, Indoor and Mobile Radio Commun. Sympos.*, Sep. 2013.

[39] D. W. K. Ng, R. Schober, and H. Alnuweiri, "Secure Layered Transmission in Multicast Systems With Wireless Information and Power Transfer," in *Proc. IEEE Intern. Commun. Conf.*, Jun. 2014, pp. 5389–5395.

[40] D. W. K. Ng and R. Schober, "Resource Allocation for Coordinated Multipoint Networks With Wireless Information and Power Transfer," in *Proc. IEEE Global Telecommun. Conf.*, Dec. 2014, pp. 4281–4287.

[41] M. Chynonova, R. Morsi, D. W. K. Ng, and R. Schober, "Optimal Multiuser Scheduling Schemes for Simultaneous Wireless Information and Power Transfer," in *23rd European Signal Process. Conf. (EUSIPCO)*, Aug. 2015.

[42] Q. Wu, M. Tao, D. W. K. Ng, W. Chen, and R. Schober, "Energy-Efficient Transmission for Wireless Powered Multiuser Communication Networks," in *Proc. IEEE Intern. Commun. Conf.*, Jun. 2015.

[43] D. Ng and R. Schober, "Max-Min Fair Wireless Energy Transfer for Secure Multiuser Communication Systems," in *IEEE Inf. Theory Workshop (ITW)*, Nov 2014, pp. 326–330.

[44] C. Valenta and G. Durgin, "Harvesting Wireless Power: Survey of Energy-Harvester Conversion Efficiency in Far-Field, Wireless Power Transfer Systems," *IEEE Microw. Mag.*, vol. 15, pp. 108–120, Jun. 2014.

[45] T. Le, K. Mayaram, and T. Fiez, "Efficient Far-Field Radio Frequency Energy Harvesting for Passively Powered Sensor Networks," *IEEE J. Solid-State Circuits*, vol. 43, pp. 1287–1302, May 2008.

[46] E. Boshkovska, "Practical Non-Linear Energy Harvesting Model and Resource Allocation in SWIPT Systems," Master's thesis, University of Erlangen-Nuremberg, 2015. [Online]. Available: http://arxiv.org/abs/1602.00833

[47] E. Boshkovska, D. W. K. Ng, N. Zlatanov, A. Koelpin, and R. Schober, "Robust Resource Allocation for MIMO Wireless Powered Communication Networks Based on a Non-linear EH Model," 2017, accepted for publication, IEEE Trans. Commun.

[48] M. Grant and S. Boyd, "CVX: Matlab Software for Disciplined Convex Programming, version 2.0 Beta," [Online] https://cvxr.com/cvx, Sep. 2013.

[49] Q. Li and W. K. Ma, "Spatically Selective Artificial-Noise Aided Transmit Optimization for MISO Multi-Eves Secrecy Rate Maximization," *IEEE Trans. Signal Process.*, vol. 61, pp. 2704–2717, May 2013.